

Gap state spectroscopy in Se-based amorphous semiconductors

V. I. MIKLA*, V.V. MIKLA^a

Institute for Solid State Physics and Chemistry, Uzhgorod National University, 88000 Uzhgorod, Voloshina 54, Ukraine
^aYazaki, Ukraine, Ltd

Thermally stimulated depolarization currents (TSDC) trap level spectroscopic technique is considered for studying of the corresponding defect states in the mobility gap in high-resistance amorphous Se-based semiconductors.

(Received February 15, 2008; accepted March 12, 2008)

Keywords: Amorphous semiconductors, Trap level spectroscopy, Thermo-stimulated depolarization

1. Introduction

Chalcogenide glasses are oxygen-free inorganic glasses containing one or more kind of chalcogen elements. As for the terminology of “amorphous” and “glassy” materials we have follow Mott and Devis (see “Electronic Processes in Non-Crystalline Materials”) and Borisova (“Glassy Semiconductors”) definitions. Accordingly, the amorphous material is a non-crystalline solid, and the glass is amorphous material produced through melt quenching. Chalcogenide glasses based on sulfides, selenide and telluride alloys in binary and multi-component systems have evolved much interest in terms of the understanding of basic physics of non-crystalline solids as well as for the development of various semiconductor devices [1-4]. Various unique phenomena are inherent for these glasses. Among these the most intriguing is the photodarkening. The latter cannot be found in crystalline chalcogenides or in any other amorphous semiconductors and are an interesting subject for fundamental research in the field of disordered materials. Reasonably, they are attractive and promising materials for various applications in modern technologies: optical memory devices, X-ray flat panel detectors, xerography, etc. [2-5]. Although a great number of studies have been undertaken to understand the characteristics of electronic and optical properties of non-crystalline semiconductors in the last three decades, many of the properties are still not clear. Some of these properties are fairly well understood, while some are still matter of debate. In this context the study of intrinsic trapping states, especially in the mobility gap of Se-based amorphous semiconductors, as we believe, is extremely important due to their technological applications.

Thermally stimulated conductivity (TSC) and thermally stimulated depolarization currents (TSDC) are a well-known techniques for obtaining data on the trapping levels of crystalline semiconductors, and the techniques have also been successfully applied to amorphous semiconductors [6-18]. The TSDC provides researchers today with an active arena of technological as well as

fundamental study. On the fundamental front, TSDC provides a powerful framework for understanding the band gap structure and properties of amorphous materials. The main attraction of TSDC as experimental method for the study of defects in high-resistance solids was, for many years, their apparent simplicity. Trapping levels in the band gap determine the fundamental electronic properties of both phases. In conventional TSC measurements difficulties arise if the thermal excitation of equilibrium carriers becomes comparable with the excitation of trapped non-equilibrium carriers. In this situation the TSC signal appears in the best case only as a shoulder on the dark current-temperature curve. One of the main difficulties in observing TSC in amorphous semiconductors is the small magnitude of the TSC currents [11,14,15,16-18]. In the most chalcogenide materials – and this may be considered even as universal property – the TSC measurements yield no peak. As for the amorphous ones, it is important to note that presently no universal method is known to detect the entire spectrum of trapping levels in the mobility gap. This is the reason why the investigators employ several complementary methods. Among these it should be mentioned those which are convenient for the study of shallow and deep trapping levels, respectively. As for the former, non-isothermal relaxation techniques and time-of flight measurements seemed to be “suitable”, as for the latter, xerographic spectroscopy is the most frequently used. Either method has its advantages and disadvantages and often it may be useful to apply the methods listed above to the same specimen. Thermally stimulated depolarization currents allow study a relaxation processes attributed to relatively shallow trapping levels. The disadvantage in measuring TSDC is the fact that the signals detected are very low and, sometimes, can be observed only in a relatively small temperature interval. At the same time, the advantage is that the TSDC method is inherently more sensitive than other methods and the resolution is usually much better. In addition, these measurements may be classified as non-destructive.

The present article reviewed our results on the extensive study of defect states in the mobility gap of amorphous As- and Sb-containing chalcogenide semiconductors by relaxation technique. For extracting typical features, elemental selenium and simple compositions with relatively low content of arsenic and antimony are exemplified as possible. We will try to attribute thermally stimulated depolarization current peaks to charge carriers release from the respective trapping levels in the band gap of these materials.

Usually, two basic types of relaxation techniques are used:

a) Isothermal relaxation: the perturbation is implemented at a constant temperature

b) Non-isothermal relaxation: the system is perturbed at a sufficiently low temperature to reduce the probability to establish a new statistical equilibrium. Subsequently, the temperature is increased according to a well-controlled heating program $T(t)$ and the relaxation of the system can be monitored as a function of temperature and time.

In the present study we emphasized on non-isothermal relaxation technique.

The occurrence of thermally stimulated depolarization current during a thermal scan of a previously excited ("perturbed") material is probably the most direct evidence we have for the existence of electronic trap levels in the band-gap of these materials. The main attraction of TSDC and related techniques as experimental methods for the study of the trapping levels in high-resistance semiconductors were their apparent simplicity. A TSDC spectrum (for historical reasons frequently referred to as "glow curve") usually consists of a number of more or less resolved peaks in current vs temperature dependence. The latter, in most cases, may be attributed to a species of traps.

Since the escape probability of carriers from trapping states is proportional to $\exp(-E_t/kT)$, the location of glow peak on the temperature scale provides information on the value of the thermal activation energy E_t . Hence, a glow curve represents a spectrum of energy required for carriers to be released from various traps in material.

2. Thermally stimulated depolarization currents in amorphous chalcogenides

2.1 Background

At the very beginning, as far as amorphous materials are concerned, it must be remembered that the validity of a pure trapping model is still a moot point. In such non-periodic structures the immobilization of charge carriers for long periods does not necessarily indicate the presence of traps, a simple alternative explanation being that the carriers are slowly moving to the extent which is determined by an inherently low-mobility process, such as hopping. At the same time, it should be noted that although chalcogenide glasses may have traps distributed throughout the mobility gap, it appears justifiably to use

the single trap approach to calculate the trapping parameters (especially activation energy) of the materials under study. In addition, such a model based on simplified version of the relaxation kinetics, as we believe, may be the commonly employed procedure in other complicated cases.

Consider first a single trap level of density M at energy E_t in the mobility gap ΔE of p-type semiconductor. The level capture cross section is S and the concentration of trapped carriers m . We assume that initially the sample is at a uniform temperature, T_0 , low enough ($T_0 \approx 80$ K) to prevent thermal emission of holes from their respective trap. Increasing the temperature according to a heating program $T(t)$ leads to release of trapped carriers until thermodynamic equilibrium is reached again at some higher temperature. Furthermore, we assume the density of equilibrium carriers p_0 substantially less than those

released from traps p_t and, besides neglecting diffusion and carrier recombination or generation, the excess charges can be considered as uniformly distributed and concentrated in narrow layers close to the electrodes (barrier type polarization), if at least one of the semiconductor-electrode interfaces can be considered as fully blocking (insulated electrode). The discharge of a photoelectret, i.e., amorphous material previously polarized by the photoelectret effect, may be expressed in the form

$$Q(T) = Q_0 \exp \left[\frac{4\pi\epsilon\mu}{\chi v_T} \int_{T_0}^T p(T) dT \right], \quad (2.1)$$

where Q_0 is the initial charge, μ the microscopic mobility, χ the permittivity of the material, p the concentration of free holes in the valence band and v_T the heating rate. The current induced in the measuring circuit by the internal field of photoelectret during heating (irreversible scan $T(t)$) is described by the equation

$$I(T) = \frac{4\pi\epsilon\mu}{\chi} Q_0 p(T) \exp \left[-\frac{4\pi\epsilon\mu}{\chi v_T} \int_{T_0}^T p(T) dT \right] \quad (2.2)$$

We may write

$$p(T) = p_0(T) + p_T(t) \text{ with } p_0(T) = C \exp \left[-\frac{\Delta E}{2kT} \right], \quad (2.3)$$

where C is the pre-exponential factor of the dark conductivity and k the Boltzmann constant.

For states distributed in energy or for N discrete states very close to each other, equation (2.3) transforms:

$$P(T) = C \exp \left[\frac{\Delta E}{kT} \right] + \sum_{i=1}^N p_{ii}(T),$$

p_0 and p_t ratio in (2.3) determine which of two factors, namely equilibrium or non-equilibrium (due to emission

from traps) carriers, dominate in relaxation process. That is the depolarization current contains two maximum: one is related to release of carriers from trap, the origin of the other lies in the change of conductivity with temperature [14-18]. Although only one of the peaks mentioned contains information about trap parameters, it is possible to discriminate between simultaneously occurring processes, e.g., thermally stimulated depolarization and thermally stimulated dielectric relaxation.

For p_i to be defined, it is necessary to solve the rate equations [19]

$$\frac{d(m+p)}{dt} = \frac{p(t)}{\tau} \tag{2.4}$$

$$\frac{dm(t)}{dt} = -\alpha(t)m(t) + \gamma[M - m(t)]p(t). \tag{2.5}$$

Here $\alpha = \gamma N_v \exp[-E_i/kT]$.

The expressions (2.1)-(2.5) are similar to those describing thermally stimulated conductivity processes obeying first-order kinetics and represents an asymmetrical glow curve the amplitude of which is a function of heating rate.

Detailed solutions have not been discussed in the literature so far. The time dependence of the rate equations (2.4) and (2.5) is replaced by the temperature dependence via the heating program, which is taken to be linear $T(t) = T_0 + v_T t$, where $v_T = dT/dt$ is the heating rate. Re-trapping can be neglected in a sample at high electric fields. From (2.4) and (2.5) we have

$$\frac{dp}{dT} = \frac{dm}{dT} + \frac{p}{v_T \tau} \tag{2.6}$$

$$\frac{dm}{dT} = \frac{\alpha(T)m(T)}{v_T} \tag{2.7}$$

and for

$$P_i(T) = \tau m(T) \gamma N_v \exp[-E_i/kT], \tag{2.8}$$

where $\gamma = \langle V \rangle S$, V is the average thermal velocity of charge carriers, S capture cross section (for neutral, attractive or repulsive centers), and N_v the density of states in the valence band. It is obvious that the only parameters markedly affecting the peak amplitude and position will be the heating rate v_T in combination with the characteristic frequency factor γN_v and the activation energy E_i .

Equation (2.2) is solved numerically with parameters $\Delta E, C, \mu, E_i, \gamma N_v$ given. It was found to be a good approximation for a wide range of physically reasonable

trapping and other parameters, typical for a wide range of amorphous semiconductors:

$$1.0eV \leq \Delta E \leq 2.0eV; \quad 10^{23} \leq C \leq 10^{30} cm^{-3};$$

$$\mu \approx 10^{-3} - 10^{-5} cm^2/Vs;$$

$$0.2eV \leq E_i \leq 0.8eV; \quad 10^7 \leq \gamma N_v \leq 10^{13} s^{-1}.$$

The capture cross section of a trap is largely determined by its charge state. Values reported in the literature (see [1] and Refs. therein) span the range 10^{-15} to $10^{-12} cm^2$ for Coulomb-attractive centers, 10^{-17} to $10^{-15} cm^2$ for neutral centers and down to $10^{-22} cm^2$ for Coulomb-repulsive centers.

Some examples of (2.2) numerical solutions are shown in Fig. 2.1. It should be emphasized here that numerical solutions of (2.2) exhibit a greater variety of shapes, peak positions and magnitudes than shown.

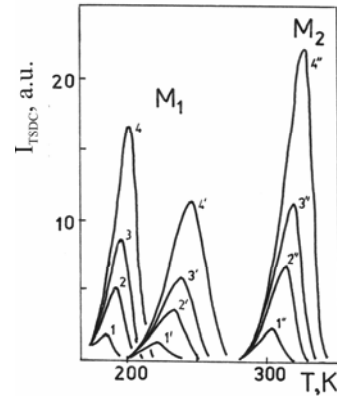


Fig. 2.1. Numerical solutions of equation (2.2) for the case $E_i = 0.4eV$ and $\gamma N_v = 10^7$ and $10^9 s^{-1}$ (curves 1-4 and 1'-4', respectively). Heating rate is 0.1, 0.3, 0.5 and 1.0 K/s^{-1} (curves 1-4, respectively). Also shown are the dielectric relaxation currents (maximum M_2) for the same heating rates (curves 1''-4'', respectively; $\Delta E = 1.8eV$, $C = 10^{25} cm^{-3}$).

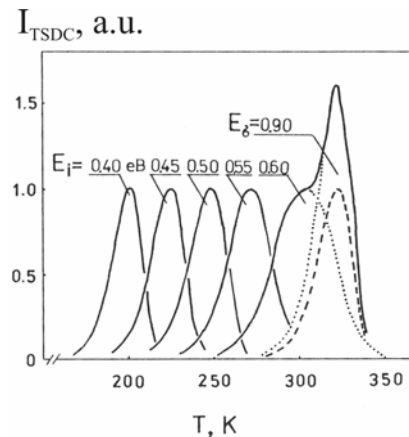


Fig. 2.2. TSDC maximum dependence on energy location of trapping level E_i . $\gamma N_v = 10^9 s^{-1}$. $0.9 eV$, $C = 10^{25} cm^{-3}$.

Although two peaks of comparable amplitude are presented (see Fig. 2.1), only the first, denoted as M_1 , is actually related to the carriers release from trap, the second, denoted as M_2 , is connected with dark conductivity variation with temperature (DC conductivity-determined relaxation peak related to the movement of equilibrium carriers).

Thus, variation of the conductivity value σ , mobility gap ΔE , and the activation energy of trap let us to establish the range where TSDC peaks directly related to traps can be observed “safely”. For example, one can detect only traps with $E_t \leq 0.6$ eV if the dielectric relaxation peak locates close to the room temperature.

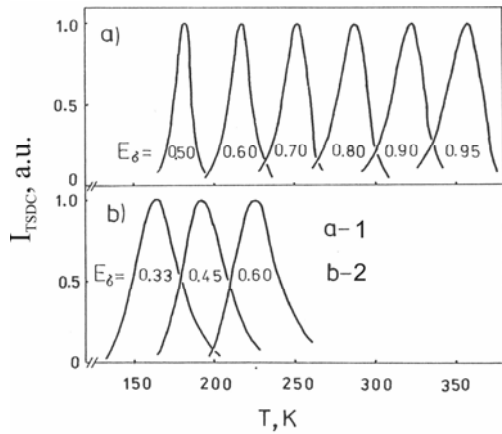


Fig. 2.3. Dielectric relaxation maximum as a function of DC conductivity activation energy E_σ . (a) and (b) denotes various activation energy values of DC conductivity.

Very illustrative for this statement are TSDC experimental results on $\text{Cu}_x(\text{As}_2\text{Se}_3)_{1-x}$ glasses. Essential increasing of dark conductivity and decreasing of its activation energy E_σ with Cu content is characteristic for these glasses. Accordingly, conductivity-determined depolarization maximum shifts to lower temperatures (Table 2.1). As for the peak associated with traps, those may be observed only in $\text{Cu}_{0.05}(\text{As}_2\text{Se}_3)_{0.95}$. In $\text{Cu}_x(\text{As}_2\text{Se}_3)_{1-x}$ glasses with $x > 0.05$ the TSDC maximum observed is simply the result of two peaks overlapping – those determined by equilibrium (dark) conductivity and, on the other hand, associated with trapping levels.

Table 2.1 Values of E_σ and E_{TSDC} * for $\text{Cu}_x(\text{As}_2\text{Se}_3)_{1-x}$ glasses.

Composition	E_σ , eV	E_{TSDC} , eV
As_2Se_3	0.91	0.89
$\text{Cu}_{0.05}(\text{As}_2\text{Se}_3)_{0.95}$	0.60	0.60
$\text{Cu}_{0.10}(\text{As}_2\text{Se}_3)_{0.90}$	0.45	0.40
$\text{Cu}_{0.15}(\text{As}_2\text{Se}_3)_{0.85}$	0.33	0.30

* E_σ and E_{TSDC} were determined from the temperature dependence of DC conductivity and TSDC curve, respectively.

The presence of maximum on the TSDC curve, which is determined by equilibrium conductivity was also confirmed in the extensive article by Agarwal, in particular for chalcogenide glasses. Moreover, it was shown that the TSDC curves may contain more than one peak, the position and amplitude of which depends on the size and relative geometrical arrangement of the electrodes with respect one to another [14].

The model presented by us has been found to fit satisfactorily the experimental data in many cases, particularly for high-resistance amorphous chalcogenide semiconductors. We have compared the calculated and experimentally observed depolarization currents for $\text{As}_{0.5}\text{Se}_{0.5}$. Two relatively broad maximum of comparable amplitude, curve shape, temperature location and similar behavior with variation of the heating rate were present on TSDC. The former (peak temperature T_{M1}) is attributed to trapping level while the latter (peak temperature T_{M2} , such that $T_{M2} > T_{M1}$) is caused by dielectric relaxation current. In fact, one of the major problems of thermally stimulated current measurements is to unequivocally determine the physical origin of the observed current peaks. This is not an easy task and a great deal of controversy still surrounds the interpretation of TSDC experimental data for most the materials tested. In our case the origin of the second peak on the depolarization curve is strongly supported by the appearance of single, close to room temperature, peak in the thermally stimulated capacitor discharge experiment. It involves filling the states located near Fermi level at some temperature (e.g., room temperature) by the application of a strong field and subsequent cooling to a lower temperature with the field applied. Then, the field is removed and the sample heated in the usual manner. The current, measured during heating, is the dielectric relaxation current. This contains information only on electronic states giving rise to dark (equilibrium) conductivity.

3. Thermally stimulated depolarization currents in Se-based amorphous semiconductors: experimental results

3.1 Sample preparation

The sample preparation is always the same, independently of the concrete measuring technique applied. Usually, the special geometry of the sample may be adapted to the circumstances desired. Special attention was on homogeneous field distribution in the sample. This allows an unambiguous interpretation of the experimental results. For any leakage currents to be avoided, the sample surfaces were carefully cleaned. Blocking electrodes have been formed simply by pressing small metal lamellae (or foil) to well polished bulk samples (amorphous film). Highly insulating spacers were put under the lamellae. Thin lead wires were attached to the electrodes and allowed

a good electrical contacts. The experiments are carried out with different electrode materials and structures with insulated electrodes. In the latter case, insulating layers are inserted between the sample and the measuring electrodes. TSDC measurements were carried out on bulk glass (sample thickness ≈ 0.5 mm) and amorphous film (thickness of ≈ 1 -10 μm) samples. The heating rate was varied by application of different voltages across the heater. Typical heating rates are in the range 0.1-1.0 K/s. At lower heating rates the current signal becomes very small, while at higher heating rates the temperature gradient inside the bulk sample causes a signal distortion.

3.2. Experimental arrangement

As a general rule, the detection efficiency expected in conventional TSC experiments will be no more than 0-15% for carrier drift. It is possible, however, to significantly increase the efficiency of TSDC by using an insulating electrode adjacent to one side of the sample (insulating foil). Since the insulating electrode blocks any charge exchange, all image charges previously induced at the non-contacting electrode (due to carriers de-trapping from gap states) will be released during the TSDC run; it will be possible also to observe the current resulting from DC conduction. We have initially assumed a well-defined sandwich-cell configuration consisting of a sample that is insulated from the metallic electrodes. The experimental apparatus used for recording TSDC is classical; it essentially composed of cryostat with sample holder, voltage supply, heater and a current detector. Standard metal-glass cryostats are used in low temperature studies of TSDC. The temperature of the films is controlled by mounting a heater inside the sample holder, and measured with thoroughly calibrated copper-constantan thermocouple. Electrical leads and feed troughs are designed for minimal leakage currents and stray capacitance. The sample was provided with a digitally controlled voltage supply of extreme stability and low noise level.

TSDC experiments are customarily analyzed assuming the sample behaves "ohmic", that is the contacts do not introduce an inhomogeneous distribution of the electric field or carrier density and a uniform bulk density of carriers extend through the entire sample. Experiments were carried out in such a way to as minimize injection effects. Contact configuration was typical for TSDC experiments. Because the currents through the sample are in almost all the cases extremely small, we have used sensitive dc ammeter (model U1-15, detection limit $\leq 10^{-15}$ A) with linear output signal. The simplest way to obtain a record of TSDC is an X-Y recorder which displays $I(T)$ and the temperature. The equipment for the extraction of trap-spectroscopic information may be connected with devices for electronic data processing. The experimental errors in E_f determination are less than 2 %.

In the TSDC considered here, a sample is cooled to a low temperature (≈ 100 K) and illuminated with 3×10^3 Lx light for a time t_p (≈ 4 min) in the presence of an

applied DC field ($E=5 \times 10^4$ V cm^{-1}). Then the light and voltage are switched off, the structure is "short-circuited" and after a delay period, necessary for sample relaxation (to reach equilibrium between the free and the trapped carriers), the sample is heated in the darkness at a constant rate ν_T while the TSDC is measured. We preferred TSDC experiments because of the absence of noise due to a voltage source, and the strongly reduced influence of the intrinsic conductivity.

3.3. TSDC in pure selenium

Conventional thermally stimulated conductivity in glassy selenium exhibit monotonic temperature dependence without distinct "structure" which is characteristic for crystalline analog. The characteristic peaks attributed to traps are usually absent on thermally stimulated conductivity vs temperature dependencies. Such a behavior is typical for chalcogenide glassy semiconductors. Although thermally stimulated conductivity exceeds the dark conductivity, the absence of a well-defined structure of the TSC does not allow identify respective trapping levels [17-19]. Therefore, another methods of thermally activation spectroscopy are needed, e.g. thermally stimulated depolarization currents.

The TSDC on glassy selenium samples start from the 'photoelectret' state. The latter is most strongly expressed at blocking electrodes. Thus, and in order to separate the TSDC peak from the DC conduction, we placed a highly insulating layer between the glass specimen and metal electrodes in the measuring cell. Two different materials were used as the dielectric insulator: cleaved mica sheet and Teflon. The two dielectric materials gave essentially the same results.

TSDC measurements on glassy selenium samples display a well-shaped, nearly symmetrical, peak at $T_m = 150$ K. It is a general fact in chalcogenide glasses (amorphous materials) that the peaks extend over a wide, comparatively to their crystalline analogs, temperature range. In addition, the peaks are flatter and more symmetrical than expected from the simple expressions (see sect. 2). For example, $\Delta T_{\text{max}}' \approx \Delta T_{\text{max}}'' = 11$ K with $\Delta T_{\text{max}}'$ and $\Delta T_{\text{max}}''$ being the half-width of the peak from the low and high temperature side, respectively. At lower heating rates ν_T , the peak shifts to lower temperatures and is reduced in heights, as expected (Fig. 3.1).

Principal trap parameter, the activation energy, can be easily calculated from a single TSDC experiment by means of some characteristic elements of the peak such as its half-width, inflection point or initial part of current rise. The most useful ones and, in fact, the most frequently exploited is undoubtedly the initial rise method (Garlick and Gibson) [20] being always easily applicable to a previously cleaned peak.

The initial rise method based on the fact that, the integral term in the $J_D(T)$ function (for details see

Ref.[9]) being negligible at $T \ll T_m$, the first exponential dominates the temperature rise of the initial current, so that

$$\ln J_D \approx \text{const.} - \frac{E}{kT} \quad (\text{Arrhenius shift}).$$

The activation energy can be determined by plotting $\ln J_D$ against $1/T$. In this approximation, a straight line is obtained, the slope of which gives $-E/k$. The method has several advantages, indeed, as it necessitates neither a linear heating rate nor a precise knowledge of the absolute temperature (it is readily seen, for example, that a thermal gradient of 5 K in a sample leads to a relative error $\Delta E/E$ less than 3% at 300 K). It is, however, somewhat limited because use of only the initial part of the curve is permitted, which may force one into the region where the uncertainty in background current is important. On the other hand, the method is still applicable for overlapping relaxation even if they cannot be isolated by cleaning, provided that a series of partial heating, each separated by rapid cooling, are performed up to gradually increasing temperatures that span the whole temperature range of the spectrum.

The activation energy E_t associated with the peak at $T_m = 150$ K has been calculated by the above method, i.e. plotting $\log I$ against $1/T$ from the initial rise of the curves. Such a plot for $v_T = 0.08 \text{ K/s}$ is shown in the inset (Fig. 3.1.). The activation energy obtained by this method is 0.22 eV.

An independent check of the correctness of the activation energy E_t can be obtained by measuring the TSDC at different heating rate v_T [21]. A number of heating rates are used and T_m is determined as a function of v_T . A plot of $\ln(T_m^2/v_T)$ against $1/T_m$ in such a case yields a straight line [22], from the slope of which the activation energy is calculated. Reasonably, the success of this method for the analysis of TSDC curves depends only how much the position of a given peak can be shifted. Therefore, the method will be applicable only when the activation energies are small. It should be noted that E_t value determined by this method is consistent with that estimated from the initial rise method.

It is necessary to note that the systematic variation in specimen thickness (between 50-500 μm) and those of different materials as the dielectric insulator yielded nearly the same peak position and activation energy. This strongly suggests that disturbing contact effects are absent. Moreover, no difference was observed between specimens open-circuited or short-circuited during cooling, nor did the time interval between irradiation and subsequent heating appear to have any affect on the observations. Therefore, it appears that the thermally stimulated depolarization currents considered here are the true TSDC associated with thermal release of non-equilibrium carriers

from localized gap states. The trap of activation energy 0.22-0.24 eV acts as a shallow trap.

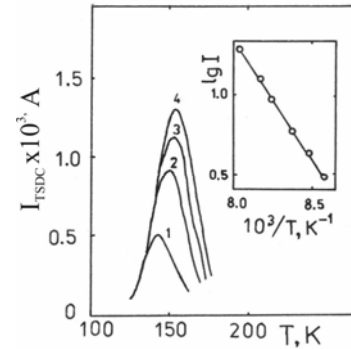


Fig. 3.1. Variation in the TSDC for various heating rates v_T in amorphous selenium: v_T is 0.08 K/s^{-1} ; 0.17 K/s^{-1} 0.23 K/s^{-1} and 0.44 K/s^{-1} (curves 1-4, respectively). The inset shows the Arrhenius plot of TSDC for curve 1.

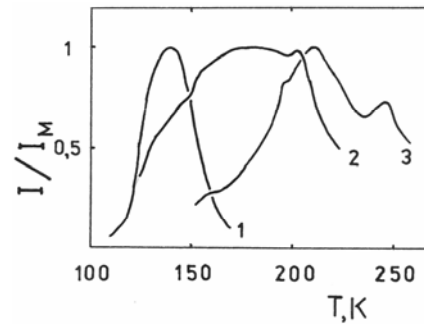


Fig. 3.2. Thermally stimulated depolarization currents in glassy Se (1), $\text{As}_{0.01}\text{Se}_{0.99}$ (2) and $\text{As}_{0.15}\text{Se}_{0.85}$ (3).

Additionally to low temperature peak at $T_{\text{max}} \approx 150 \text{ K}$, a peak at $T_{\text{max}} \sim 270 \text{ K}$ (not shown in Fig.3.1) is also present on the TSDC curve. The ratio of amplitudes of these two, low and high temperature peak, is ~ 5 . It is important to note here that the dielectric relaxation current peak (in the depolarization of thermoelectret state experiments) at $T_{\text{max}} \sim 270 \text{ K}$ is also observed. The activation energy determined for this peak is $\sim 0.60 \text{ eV}$. Essentially, this parameter shows dependence on electrodes configuration and sample thickness. Therefore, a peak with $T_{\text{max}} \sim 270 \text{ K}$, may be attributed simply to the change in dark conductivity with temperature.

3.4. TSDC in $\text{As}(\text{Sb})_x\text{Se}_{1-x}$ alloys

Arsenic addition, even in a relatively low as for glassy compounds amount (~ 1 at %), to amorphous selenium causes a change in the shape of TSDC curve. As it illustrates Fig. 3.2, transition from pure amorphous Se to $\text{As}_{0.01}\text{Se}_{0.99}$ accompanied by the broadening of the

corresponding TSDC curve and appearance of additional maximum.

The main maximum on the depolarization curve is shifted respectively to those observed in a-Se and locates in the range 190-200 K. This maximum is the result of overlapping of two maximum with $T_{max} \approx 191$ K and $T_{max} \approx 203$ K. In addition, the shoulder at 160 K is also observed. The shoulder and the peak position observed in pure selenium correlate. For the separation of the overlapping maximum, the method of partial thermal cleaning was used. The method is based on the release of carriers from traps by heating sequences to the temperatures higher than T_{max} of corresponding maximum, rapid cooling and heating again. The result obtained after applying such a procedure to $As_{0.01}Se_{0.99}$ is shown in Fig. 3.3.

Values of activation energy calculated by the initial rise method are in the range $0.25 \div 0.45$ eV. Continuous distribution of localized states in this range was confirmed by increasing of activation energy in a sequence - curve 2-4 (Fig. 3.3.).

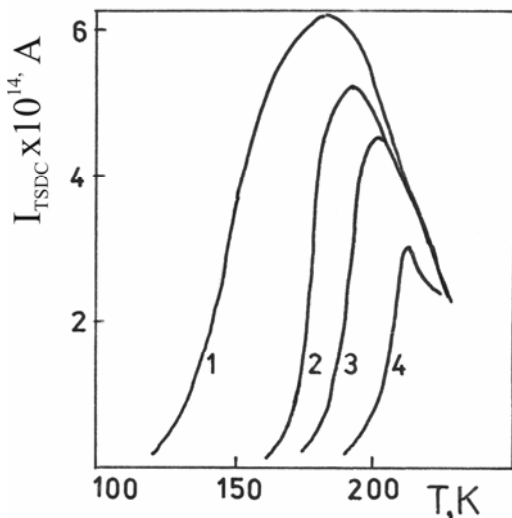


Fig. 3.3. Application of thermal cleaning method of TSDC peaks to $As_{0.01}Se_{0.99}$. 1 - Initial TSDC curve. The temperature in the successive cycles of heating is 166 K (2), 180 K (3) and 199 K (4).

Further increasing of As addition (up to 6 at %) does not change the shape of TSDC curve: the latter remains similar to that observed in $As_{0.01}Se_{0.99}$.

In Fig. 3.4, the TSDC observed in As_xSe_{1-x} for As content 8-15 at % was shown. A peak at $T_{max} \approx 210$ K dominates in the depolarization curve. In addition, a peak at $T_{max} \approx 244$ K and a shoulder at $T_{max} \approx 197$ K is discernible. Release of carriers from shallow states and subsequent trapping on relatively deeper ones transforms the TSDC into the curves 3 and 4 (Fig. 3.4.). The activation energy determined for the peaks with $T_{max} \approx 210$ K and $T_{max} \approx 244$ K is $E_{i2} = 0.35$ eV and $E_{i3} = 0.45$ eV. These states are energetically distributed: $\Delta E_{i2} = 0.05$ eV and $\Delta E_{i3} = 0.1$ eV, respectively.

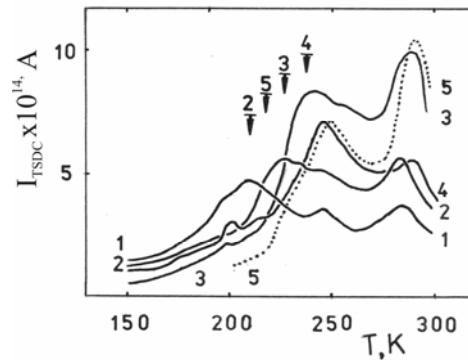


Fig. 3.4. TSDC curves of $As_{0.15}Se_{0.85}$ samples (1). Curves 2-5 - polarized samples were heated under applied DC voltage to the temperatures shown by arrows.

In Fig. 3.4, the TSDC observed in As_xSe_{1-x} for As content 8-15 at % was shown. A peak at $T_{max} \approx 210$ K dominates in the depolarization curve. In addition, a peak at $T_{max} \approx 244$ K and a shoulder at $T_{max} \approx 197$ K is discernible. Release of carriers from shallow states and subsequent trapping on relatively deeper ones transforms the TSDC into the curves 3 and 4 (Fig. 3.4.). Activation energy determined for peaks with $T_{max} \approx 210$ K and $T_{max} \approx 244$ K is $E_{i2} = 0.35$ eV and $E_{i3} = 0.45$ eV. These states are energetically distributed: $\Delta E_{i2} = 0.05$ eV and $\Delta E_{i3} = 0.1$ eV, respectively.

For TSDC in Sb_xSe_{1-x} alloys, we have three peaks M_1 , M_2 and M_3 whose temperatures T_{M1} , T_{M2} and T_{M3} (145, 175 and 195 K, respectively) are close enough to each other that they overlap (Fig. 3.5.). The TSDC method allows the easy and quick resolution of the overall spectrum, in our case peaks 1, 2 and 3. There are two ways in which this can be done.

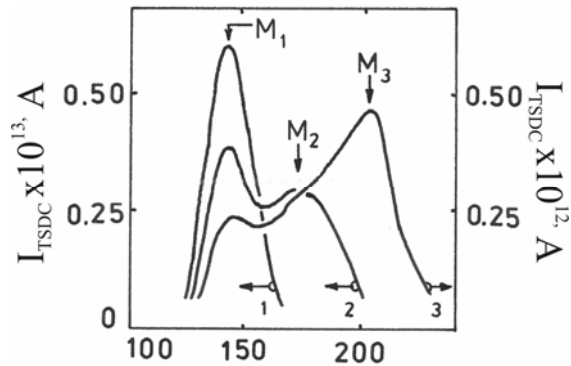


Fig. 3.5. TSDC spectra of Sb_xSe_{1-x} . $x = 0$ (1), 0.01 (2), 0.05 (3).

The first method, common to all non-isothermal techniques, was developed by Greswell and Perlman [22]. Suppose, for example, we have two peaks 1 and 2, whose temperatures T_{m1} and T_{m2} ($T_{m1} < T_{m2}$) are close enough to each other as to overlap. After the whole TSDC curve has been obtained, a second thermal cycle is started. However, instead of recording the discharge at one time, it

is firstly discharged the lower temperature peak 1 by heating until T_a ($T_{m1} < T_a < T_{m2}$), then cooling the sample again and finally one obtains the discharge of peak 2, which is “pure” or nearly “pure”.

The second cleaning method, specific to TSDC measurements and which may be applied in our case, is due to Bucci et al. [23]. It consists of first polarizing the material at a temperature T_b such that $T_{m1} < T_b < T_{m2}$ for an interval of time $\tau_1(T_b) \ll \tau_2(T_b)$: the resulting TSDC curve will then show only peak 1. Peak 2 can also be isolated in a similar way by using $T_c > T_{m2}$ and removing the field at temperature T_d such that $T_{m1} < T_d < T_{m2}$.

Such an effective way of separating the above-mentioned peaks is illustrated in Fig. 3.6.

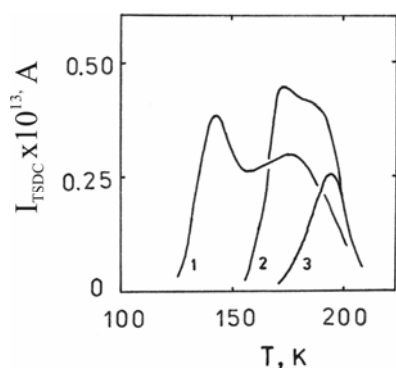


Fig. 3.6. Thermal cleaning procedure (of TSDC) applied to $Sb_{0.01}Se_{0.99}$. 1 – the whole TSDC curve. For curves 2 and 3, $T_a=165$ K and $T_b=195$ K (see the text).

The activation energies determined by these methods were $E_{t1}=0.22$ eV, $E_{t2}=0.34$ eV and $E_{t3}=0.45$ eV. Note that some of the above traps in the materials studied were “visible” in time-of-flight and xerographic experiments [5,17,19].

Concluding remarks

The results taken as a whole reveal the existence of at least three different trap species in the band-gap of $Sb(As)_xSe_{1-x}$ non-crystalline semiconductors. These species are located at energies 0.22, 0.34 and 0.45 eV, respectively, below the conduction band edge and control the electron transport properties of the material. It seemed that Sb and As introduced a new set of detectable charge carrier traps.

Space considerations precluded a detailed discussion of the similar trapping levels in other high-resistance amorphous chalcogenides.

Finally, we are convinced that the future development of TSC and TSDC methods as investigative tools of electronic properties of amorphous semiconductors will

benefit from similar skillful studies via time-of-flight and xerographic measurements.

References

- [1] M. Popescu, J. Non-Cryst. Solids **352**, 887 (2006).
- [2] A. V. Kolobov (ed.) Photoinduced Metastability in Amorphous Semiconductors, Wiley-VCH, Weinheim (2003).
- [3] J. Singh, K. Shimakawa, Advances in Amorphous Semiconductors, Taylor and Francis, London (2003).
- [4] G. Lucovsky, M. Popescu, Non-Crystalline Materials for Optoelectronics, INOE Publishers, Bucharest (2004).
- [5] S. O. Kasap, in “Handbook of Imaging Materials” edited by A.S. Diamond and D.S. Weiss (Marcel Dekker, Inc., New York, Second Addition, New York, 2002).
- [6] D. Kumar, S. Kumar, Chalcogenide Letters **1**, 49 (2004).
- [7] E. Skordeva, J. Optoelectron. Adv. Mater. **3**, 437 (2001).
- [8] V. F. Zolotaryov, D. G. Semak, D. V. Chepur, Phys. Status Solidi **21**, 437 (1967).
- [9] P. Braunlich, P. Kelly, J. P. Fillard, Thermally Stimulated Relaxation in Solids (Top. Appl. Phys. **37**) ed. P. Braunlich (Springer, Berlin, 1979).
- [10] Yu. Gorokhovatsky, G. Bordovskij, Thermally Activational Current Spectroscopy of High-Resistance Semiconductors and Dielectrics (Nauka, Moscow, 1991) (in Russian).
- [11] R. A. Street, A. D. Yoffe, Thin Solid Films **11**, 161 (1972).
- [12] B. T. Kolomiets, V. M. Lyubin, V. L. Averjanov, Mater. Res. Bull. **5**, 655 (1970).
- [13] T. Botila, H. K. Henish, Phys. Status Solidi (a) **36**, 331 (1976).
- [14] S. C. Agarwal, Phys. Rev. B **10**, 4340 (1974).
- [15] S. C. Agarwal, H. Fritzsche, Phys. Rev. B **10**, 4351 (1974).
- [16] P. Muller, Phys. Status Solidi (a) **67**, 11 (1981).
- [17] V. I. Mikla, Dr. Sci. Thesis, Institute of Physics, National academy of Sciences, Kiev (1998).
- [18] A. A. Kikineshi, V. I. Mikla, I. P. Mikhalko, Sov. Phys.-Semicond. **11**, 1010 (1977).
- [19] V. I. Mikla, I. P. Mikhalko, Yu. Yu. Nagy, J. Phys.: Condens. Matter **6**, 8269 (1994).
- [20] G. F. Garlick, A. F. Gibson, Proc. Phys. Soc. **60**, 574 (1948).
- [21] A. H. Bohun, Can. J. Chem. **32**, 214 (1954).
- [22] R. A. Greswell, M. M. Perlman, J. Appl. Phys. **41**, 2365 (1970).
- [23] C. Bucci, R. Fieschi, G. Guidy, Phys. Rev. **148**, 816 (1966).

*Corresponding author: mikla_@ukr.net